



Egyptian Journal of Cell and Tissue Research

Print ISSN: 2812-5436 / Online ISSN: 2812-5444



The Protective Effect of L-Arginine against Aspartame-Induced Toxicity on Adrenal Cortex of Adult Male Albino Rats: Histological, Immunohistochemical, and Biochemical Study

Mai Amin Al-Motasem¹, Dalia Hussein Abdelaziz Helmy², Salwa Khaled Mostafa³, Amira Shaban Gaeidy¹.

¹Lecturer of Medical Histology & Cell Biology, Faculty of Medicine, Beni-Suef University

²Professor of Medical Histology & Cell Biology, Faculty of Medicine, Beni-Suef University

³Demonstrator of Medical Histology & Cell Biology, Faculty of Medicine, Beni-suef University

Abstract:

Background: Aspartame is widely consumed worldwide. Its metabolites can be toxic to various body organs. L-Arginine is widely available in daily food products and it has an antioxidant property. **Aim:** This study was done to evaluate the protective effect of L-arginine on aspartame treated adrenal gland in a rat model using histological, immunohistochemical, biochemical, and morphometric studies. **Material and Methods:** Fifty adult male albino rats five-six month old, weighing 180-200 grams were used. They were divided into five groups. Group I (Control). Group II (L-arginine): each rat received 0.3mg/ gm/day for 4 weeks. Group III (Aspartame group): each rat received 250mg/Kg/day for 4 weeks. Group IV (Aspartame+L-arginine treated group) each rat received L-arginine & aspartame as in groups II & III respectively. Group V (Recovery group): each rat received aspartame as in group III, then, rats were left for another 4 weeks before they were sacrificed. Adrenal glands were dissected and subjected to Hematoxylin & Eosin and Masson's Trichrome stains, Caspase-3, biochemical and morphometric studies. **Results:** In aspartame group, the adrenal cortex revealed decreased capsular thickness with complete shedding in some areas by Masson's Trichrome, disorganization of the cellular arrangement in adrenal cortex. Some cells revealed vacuolated cytoplasm, others appeared with pyknotic nuclei by

Hematoxylin&Eosin.ACTH, cortisol, aldosterone, and MDA concentrations were significantly increased while GSH concentration was significantly decreased in aspartame group. Aspartame group showed significant increase in positive immunoreactivity for Caspase-3, compared to other groups. L-arginine treatment improved the histological, immunohistochemical, biochemical, and morphometric results. Recovery group (V) revealed incomplete improvement. **Conclusion:** L-arginineprotects the adrenal cortex from the aspartame induced toxicity inadult male albino rats. **Key Words:**Adrenal Cortex, L-arginine, Aspartame, immunohistochemistry, Biochemistry.

1. Introduction:

As one of the primary endocrine glands, the adrenal gland is involved in numerous aspects of physiological functions as well as stress management (1). Adrenal hormones have direct impacts on the regulation of body metabolism, so influencing the functional status of the organs and controlling the body haemostasis (2).

Toxicological studies have classified the adrenal gland as one of the highest vulnerable endocrine organs to toxic effect of chemical substances, which can alter both its structure and function (3).

Nowadays there is a raised concern about the safety of food additives that are widely used in food sweetening and enhancing flavour. One of these additives is aspartame, the non-nutritive synthetic sweetenerwith sweetening power 200 times more than that of sucrose, but with the same caloric intake, this makes the aspartame

widely consumed worldwide in hundreds of food products and pharmaceuticals used in controlling the overweightness and diabetes (4).

Even though Food and Drug Administration (FDA) agent certified aspartame's utilization, various studies on experimental animals have been carried to document aspartame's hazardous effects and associated pathological conditions such as increasing the incidence of diabetes type II, nephrotoxicity, liver toxicity, and neurological disturbance. In addition to the possible carcinogenic effect (5). The worry from aspartame come from its metabolites as each of these components can be toxic to the various body organs (4).

Oxidative stress is defined as an imbalance between production of oxidants and antioxidant defences that may result in biological systems' damage (6). To defend

against oxidative stress injury, our body have evolved defence system primarily dependent upon natural antioxidant agents, in addition to other multiple antioxidant therapies(7).

Measurement of oxidative molecules can be suggestive for the occurrence of oxidative stress, as well as the effectiveness of the clinical therapies. Most of oxidative markers can be assessed in the blood plasma through ELISA kits such as Malondialdehyde (MDA), Myeloperoxidase (MPO) and antioxidant markers such as Super oxide dismutase (SOD) and Glutathione Peroxidase (GPx)(8)(9) (10).

L-Arginine, a fundamental, natural semi-essential amino acid, is widely available in

2. Materials and Methods:

Animals:

The study was performed in the animal house of Faculty of Veterinary medicine, Beni-suef University. Fifty adult male albino rats 5 to 6 months old, weighing 180-200g were used. To prevent any impact of female hormones on the activities of the adrenal gland, this study only used male rats. Each group had access to free food and was housed in a separate, sanitary cage with five rats per cage in a room with controlled lighting and temperature (22–24 °C). Rats were housed

daily food products, including wheat flour, dairy products, and nut(11). It is also regarded as a natural component of dietary proteins (12). In addition to its role in protein metabolism, L-Arginine has an antioxidant property that has been well documented in several studies through enhancing the antioxidant defence system including SOD with another indirect antioxidant effect through the generation of nitric oxide (NO) (13).

Hence, this study was done to evaluate the possible protective effect of L-arginine on aspartame treated adrenal gland in a rat model using histological, immunohistochemical, biochemical and morphometric studies.

for a week prior to the experiment's commencement and fed the standard commercial pellet diet.

This experiment was accepted by the Institutional Animal Care and Use Committee of Beni-Suef University (BSU-IACUC) (Approval Number. 022-260).

Drugs:

1. **Aspartame** was purchased from Al Ameriya Pharma Company, Egypt in form of tablets, (Trade name Diet-sweet). Each tablet contains 20 mg aspartame.

2. **L-arginine** was purchased from DOP organic Kimya Company, Turkey in form

of powder. Each 1 gm of L-arginine powder dissolved in 1 ml distilled water.

Rats were divided randomly to 5 groups (10 rats each):

Group I (10 rats): Used as control and were given distilled water only for 4 weeks.

Group II (10 rats) (L-Arginine group): Each rat received 0.3mg/gm/day prepared in distilled water and given by gastric gavage method for 4 weeks (1).

Group III (10 rats) (Aspartame group): Each rat received 250mg/Kg/day prepared in distilled water and given by gastric gavage method for 4 weeks (14).

Group IV (10 rats) (Aspartame + L-Arginine treated group): Each rat received L-arginine in the same dose, period, and route of administration of the group II concurrently with aspartame in both the same dose and route of group III for 4 weeks(1)(14).

Group V (10 rats) (Recovery group): Each rat received aspartame as in group III. Then, rats were left for another 4 weeks after cessation of aspartame administration in order to recover before they were sacrificed (15).

Methods:

At the last day of the experiment, rats were anesthetized using ether inhalation, sacrificed, carefully dissected, and adrenal

glands were taken for light and immunohistochemical examination.

Preparation of the specimens for light microscopic examination:

The obtained specimens were fixed directly in 10% formal saline then washed and dehydrated in ascending grades of alcohol (70, 90, and 100%), followed by clearing in xylene. Embedding was done and paraffin blocks were taken. Then thick serial sections (5-6 µm) were cut and mounted on glass slides. **These sections were subjected for the following:**

I- Histological study:

- 1- Hematoxylin and eosin (H&E) to demonstrate histological changes(16).
- 2- Masson's Trichrome stain to demonstrate the alterations in collagen depositions (16).

II- Immunohistochemical study:

Immunohistochemical staining with anti-caspase 3: It is an apoptotic marker. Positive reactions appear as cytoplasmic with some nuclear brown colour.

Sections for immunohistochemical stains were put in a Coplin jar with 10mM sodium citrate buffer at pH 6.0 in a microwave oven for 2 minutes for antigen retrieval. Then allowed to cool for 20 minutes at room temperature. 2-3 drops of **Caspase-3 antibody**, which is Rabbit polyclonal antibody (Diagnostic BioSystems, Cat#

PR096, USA.) were added on each slide. The slides were left for 45 minutes in the humidity chamber at room temperature then detection was performed using 2-3 drops of secondary antibody (biotinylated polyvalent) followed by colorimetric detection using DAB Kit. Sections were then counterstained with Mayer's hematoxylin, dehydrated, cleared, and mounted. Negative control was handled in the previously mentioned cycle, but with omitting the steps of adding the primary antibodies. Positive control was human tonsil that appeared as nuclear with some cytoplasmic brown deposits (17).

III- Biochemical study:

Before the rats were sacrificed, blood samples from their tail veins were collected to measure the levels of MDA, reduced glutathione (GSH), ACTH, cortisone, and aldosterone (18). Blood samples were centrifuged for 10 minutes at 3000 rpm at room temperature, then stored at -20 °C until they were analyzed. These measurements were done at the Biochemistry and Molecular Biology unit, Medical Biochemistry department, Faculty of Medicine, Cairo University.

1- Measurement of Plasma Malondialdehyde level:

IV- Morphometric Study:

Levels of MDA were expressed as nmol/ml and tetraethoxypropane was used for calibration. Kits were purchased from Bio diagnostic company, Cat#MD 25 28, Egypt.

2- Measurement of Plasma Reduced Glutathione Level:

GSH levels were measured from the standard calibration curve and expressed as mmol/L. Kits were purchased from Bio diagnostic company, Cat#GR 25 10, Egypt.

3- Measurement of Plasma ACTH Level:

ACTH levels were measured from standard calibration curve and expressed as Pg/ml. Kits were purchased from Mybiosource Company, Cat # MBS453311, USA.

4- Measurement of plasma Cortisol level:

Cortisol levels were measured from standard calibration curve and expressed as ng/ml. Cortisol ELISA kits were obtained from Cusabio Company, Cat# CSB-E05112r, USA.

5- Measurement of plasma Aldosterone level:

Aldosterone levels were measured from standard calibration curve and expressed as Pg/ml. Aldosterone ELISA Kits were obtained from abcam Company, Cat#ab136933, USA.

The following parameters were measured:

1-Measurement of the thickness of Zona

Fasciculata (ZF) in H&E sections at (X200) magnification in all groups.

2-Measurement of the mean area percentage of collagen fibers in Masson's Trichome-stained sections at (X400) magnification in all groups.

3-Measurement of the mean area percentage of Caspase-3 positive immune-reaction in immunohistochemically stained sections at (X400) magnification in all groups.

All measurements were taken using the image analyzer (Leica Q 500 MC program, Wetzlar, Germany) at Histology Department, Faculty of Veterinary Medicine, Beni-Suef University, Egypt. Examinations were performed in 5 high-power fields X400/five different sections of each rat. All these morphometrically measured data were statistically analysed.

V- Statistical Study:

All data were expressed as mean \pm SD. A histogram was created, and a student t-test was used for the statistical analysis to compare the means of the different groups. The degree of significance was estimated using the Graph Pad Software programme (San Diego, California, USA), and it was written as follows: $>P$ 0.05 is considered significant; $<P$ 0.05 is considered non-significant(14).

3. Results:

(I) Histological results:

Haematoxylin and Eosin:

Group I (Control) revealed normal histoarchitecture of the adrenal gland formed of a dense fibrous connective tissue capsule, surrounding the parenchyma. The adrenal cortex was formed of 3 zones from outside inwards: Zona Glomerulosa (ZG), Zona Fasciculata (ZF) and Zona Reticularis (ZR) **Fig. (1a)**. In **group II** (L-arginine-treated), adrenal cortex sections revealed the three zones of the adrenal cortex (ZG, ZF & ZR) which appeared comparable to group I. Fibrous CT capsule covered with adipose CT was observed. ZG arranged in oval clusters **Fig. (1b)**. Zona Glomerulosa (ZG) arranged in oval clusters of closely packed cells exhibiting pale vacuolated cytoplasm and darkly stained nuclei (thick yellow arrow). ZG is located just under the adrenal gland capsule **Fig. (1c)**. **Group III** (Aspartame-treated) showed apparent structural changes in the adrenal cortex in the form of apparent decrease in the thickness of the C.T. capsule, which appeared detached in some areas. Disorganization of the cellular arrangement in the 3 zones of the adrenal cortex was observed **Fig. (2a)**. Some sections showed distortion of the CT capsule with complete shedding in some areas.

Subcapsular dilated and congested blood vessel with some inflammatory cells was also noticed. Cells of ZG were irregularly arranged and lost its histoarchitectural pattern; some cells revealed vacuolated cytoplasm while others appeared with darkly stained pyknotic nuclei. Irregular shaped nuclei were also observed. Widened intercellular space was noticed **Fig. (2b)**. ZF exhibited an increase in its thickness. Some fields exhibited complete disruption of the normal histological architecture of ZF cells; the cells were irregularly arranged, appeared large, pale with markedly vacuolated cytoplasm and eccentric shrunken nuclei **Fig. (2c)**. In other sections, the cells of ZF exhibited deeply acidophilic cytoplasm and darkly stained nuclei. Wide areas of intercellular spaces were filled with pink eosinophilic homogenous exudate **Fig. (2d)**. In some sections, marked disruption of the normal histological architecture of the cells of the Zona Fasciculata (ZF) was noticed. Cells are irregularly arranged; some cells are shrunken exhibit deeply eosinophilic cytoplasm and pyknotic condensed nuclei. Other cells exhibit irregularly shaped nuclei. Complete dissolution of the nuclei of other cells was noted **Fig. (2e)**.

Group IV (L-Arginine and Aspartame-treated group) revealed apparent improvement in the histoarchitecture of the adrenal cortex as compared to rats receiving aspartame in group III. The adrenal cortex exhibited normal architecture with well demarcated three cortical zones; ZG, ZF and ZR. The capsule appeared restored and uniform in all parts of the adrenal gland, with overlying fat cells **Fig. (3a)**. Most of ZG cells were arranged in round clusters of closely packed cells with vacuolated acidophilic cytoplasm & deeply stained central nuclei. Restored capsule was also detected **Fig. (3b)**. The ZF regained most of its normal histological architecture, the cells were arranged in regular longitudinal cords with pale acidophilic cytoplasm and central rounded nuclei, some binucleated cells were also detected **Fig. (3c)**. **Group V** (recovery group) revealed persistence of some apparent adrenal cortical structural changes that occurred in aspartame-group. The capsule appeared normal; however, an area of capsular detachment was detected **Fig. (3d)**. Layers of adrenal cortex; especially ZF, showed apparent disorganization of their histo-architecture. Cells were shrunken with disturbed cell membranes and deeply acidophilic cytoplasm. Some cells exhibited pyknotic nuclei and others showed

karyolysis **Fig.(3e)**. Cells of ZG appeared shrunken and disarranged with acidophilic cytoplasm and pyknotic nuclei. Disturbed cell membranes and widened intercellular spaces were also noticed **Fig.(3f)**. Regarding ZF, some sections showed restoration of the cell arrangement, the cells had pale acidophilic cytoplasm and central rounded nuclei, arranged in cords with longitudinal blood capillaries in-between, but some pyknotic nuclei were still observed **Fig. (3g)**.

Masson's trichrome stained sections:

Examination of Masson's trichrome stained adrenal cortical sections of **group I** showed a uniform regular thick CT capsule formed of well-packed collagen fibres surrounding the gland. Thin C.T. trabeculae were extended from the capsule into the parenchyma of the gland **Fig. (4a)**. In **group II** histological features, comparable to those found in **group I**, were seen **Fig. (4b)**. Histological examination of adrenal cortical sections in **group III** showed distortion & separation of the capsule with apparent decrease in its thickness, compared to sections in groups I & II. Thin C.T. trabeculae were extended from the capsule into the parenchyma of the gland. Marked subcapsular blood vessels congestion was noted **Fig. (4c)**. **Group IV** showed regular, continuous CT capsule formed of well-

packed collagen fibres. The capsule exhibited apparently increased thickness, as compared to aspartame group. Thin C.T. trabeculae were extended from the capsule into the parenchyma of the gland **Fig. (4d)**. **Group V** showed that the fibrous C.T. capsule appeared relatively thick, formed of well packed collagen fibres in some areas, while in other areas, the capsule exhibited apparently decreased thickness. Very thin C.T. trabeculae extended from the capsule into the parenchyma of the gland. Marked subcapsular blood vessel congestion was also noted **Fig. (4e)**.

Anti-Caspase 3 immunostained sections:

As regards negative control; it showed no any immunohistochemical reaction for caspase-3 (Fig. 5*).

Caspase-3 immunohistochemical, stained adrenal cortical sections of **group I** showed minimal positive nuclear and cytoplasmic immune-reactions **Fig. (5a)**. In **group II**, Caspase-3 immunohistochemical, stained adrenal cortical sections showed negative immune-reactivity **Fig. (5b)**. Caspase-3 immunohistochemical, stained adrenal cortical sections of **group III** showed numerous positive nuclear and cytoplasmic immune-reactions **Fig.(5c)**. Caspase-3 immunohistochemical, stained adrenal cortical sections of **group IV** showed

minimal positive nuclear and cytoplasmic immune-reactions **Fig. (5d)**. Caspase-3 immunohistochemical, stained adrenal cortical sections of **group V** showed numerous positive nuclear and cytoplasmic immune-reactions **Fig. (5e)**.

(II) Biochemical results:

(1) The mean serum cortisol, aldosterone, and ACTH: Group III (Aspartame group) showed a significant ($P < 0.05$) increase in the mean serum **cortisol, aldosterone, and ACTH** levels as compared with group I, group II, group IV, and group V. However, **group IV (Aspartame and L-arginine)** showed significant ($P < 0.05$) decrease in mean serum **cortisol, aldosterone, and ACTH** levels as compared with group III and group V and significant ($P < 0.05$) increase as compared with group I and group II (**Table 1, Histogram 1**).

(2) The mean serum malondialdehyde (MDA) and reduced glutathione (GSH): Group III (Aspartame group) showed a significant ($P < 0.05$) increase in the mean serum **MDA** level as compared with group I, group II, group IV, and group V. However, **group IV** showed significant ($P < 0.05$) decrease in mean serum **MDA** level as compared with group III and group V and significant ($P < 0.05$) increase as compared with group I and group II. At the same time, **Group III** showed a significant ($P < 0.05$) decrease in

the mean serum **GSH** level as compared with group I, group II, group IV, and group V. However, **group IV** showed a significant ($P < 0.05$) increase in mean serum **GSH** level as compared with group III and group V and significant ($P < 0.05$) decrease as compared with group I and group II (**Table 2, Histogram 2**).

(III) Morphometric and statistical analysis:

(1) The mean Thickness of ZF in H& E-stained sections in μm : Group III (Aspartame group) showed a significant ($P < 0.05$) increase in the mean **thickness of ZF** as compared with group I, group II, group IV, and group V. However, **group IV** showed significant ($P < 0.05$) decrease in mean **thickness of ZF** as compared with group III (Aspartame) and group V (Recovery) and significant ($P < 0.05$) increase as compared with group I and group II (**Table 3, Histogram 3**).

(2) The mean area percentage of (%) collagen fibres content in Masson's Trichrome-stained sections: Group III showed a significant ($P < 0.05$) decrease in the mean **area percentage of collagen fibres content** as compared with group I, group II, group IV, and group V. However, **group IV** showed significant ($P < 0.05$) increase in mean **area percentage of**

collagen fibres content as compared with group III and group V and significant ($P < 0.05$) decrease as compared with group I and group II (L-A (Table 3, Histogram 3)).

(3) The mean area percentage of caspase-3 positive immune reaction: Group III showed a significant ($P < 0.05$) increase in the mean area percentage of caspase-3 positive immunoreaction as compared with

group I, group II, group IV, and group V. However, **group IV** showed a significant ($P < 0.05$) decrease in mean area percentage of caspase-3 positive immunereaction as compared with group III and group V and a significant ($P < 0.05$) increase as compared with group I and group II (Table 4, Histogram 4).

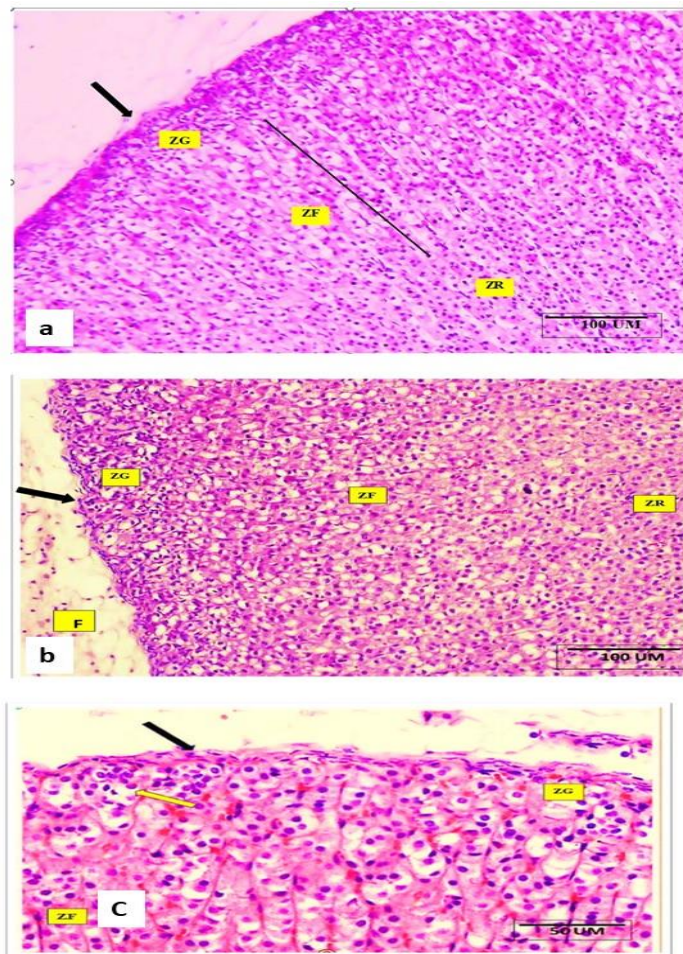


Fig. (1):(1a)A photomicrograph of H&E-stained sections of the adrenal cortex from group I (Control group) showing normal histological architecture of the adrenal cortex, consisting of 3 distinct zones: Zona glomerulosa (ZG), Zona fasciculata (ZF), and Zona reticularis (ZR). The adrenal gland was surrounded by a fibrous connective tissue capsule (thick black arrow) (Scale bar 100 μm)(H&E x200).(1b)A photomicrograph of H&E-section in the adrenal cortex of group II (L-arginine group) showing a fibrous CT capsule (thick black arrow) surrounded by fat cells (F), normal architecture of the 3 zones of the adrenal cortex; ZG, ZF and ZR was apparent(Scale bar 100 μm) (H&E x200). (1c)A photomicrograph of H&E-stained sections in the adrenal cortex of group II showing Zona Glomerulosa (ZG) arranged in oval clusters of closely packed cells exhibiting pale vacuolated cytoplasm and darkly stained nuclei (thick yellow arrow). ZG was located just under the adrenal gland capsule (thick black arrow) (Scale bar 50 μm) (H&E x400).

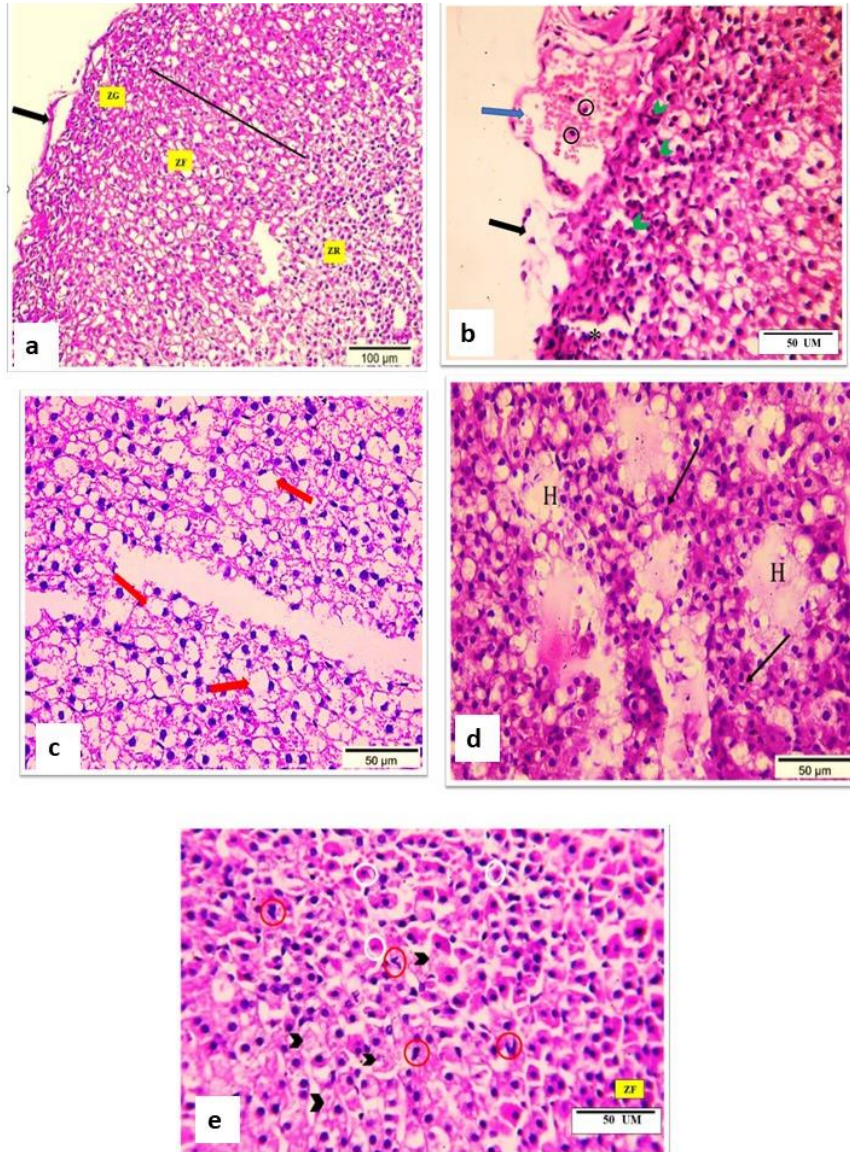


Fig. (2):(2a)A photomicrograph of a section of the adrenal cortex of group III (aspartame group) showing an apparently thin CT capsule, detached in some areas (thick black arrow). Disorganization of the cells in the three zones was apparent (ZG: Zona Glomerulosa, ZF: Zona Fasciculate and ZR: Zona Reticularis) (Scale bar 100 μ m)(H&E X200). (2b)A photomicrograph of a section of the adrenal cortex of group III showing distorted capsule with areas of complete shedding (thick black arrow),subcapsular dilated and congested blood vessel (thick blue arrow) with some inflammatory cells (black circles),disruption of the histoarchitectural pattern of Zona glomerulosa (ZG), some cells show cytoplasmic vacuolation (thin black arrows) and others showed pyknotic nuclei (white circles), and some irregular shaped nuclei (green arrow heads). Notice widened intercellular space (*) (Scale bar 50 μ m)(H&E X400). (2c)A photomicrograph of

a section of the adrenal cortex from group III showing Zona Fasciculata (ZF) with irregularly arranged cells & lost its cord pattern. The cells appeared large, pale with markedly vacuolated cytoplasm and eccentric nuclei (thick red arrows) (Scale bar 50 μm)(H&E X400). **(2d)**A photomicrograph of a section of the adrenal cortex of group III showing loss of the cord arrangement of the cells of Zona Fasciculata (ZF). The cells exhibited deeply acidophilic cytoplasm and darkly stained nuclei (black arrows), and wide areas in the intercellular spaces were filled with pink eosinophilic homogeneous material (Scale bar 50 μm)(H&E X400). **(2e)**A photomicrograph of section of the adrenal cortex from group III showing marked disruption of the normal histological architecture of the cells of the Zona Fasciculata (ZF). Cells were irregularly arranged; some cells were shrunken exhibited deeply eosinophilic cytoplasm and pyknotic condensed nuclei (white circles), other cells exhibited irregularly shaped nuclei (red circles), and complete dissolution of the nuclei of other cells (Scale bar 50 μm)(H&E X400).

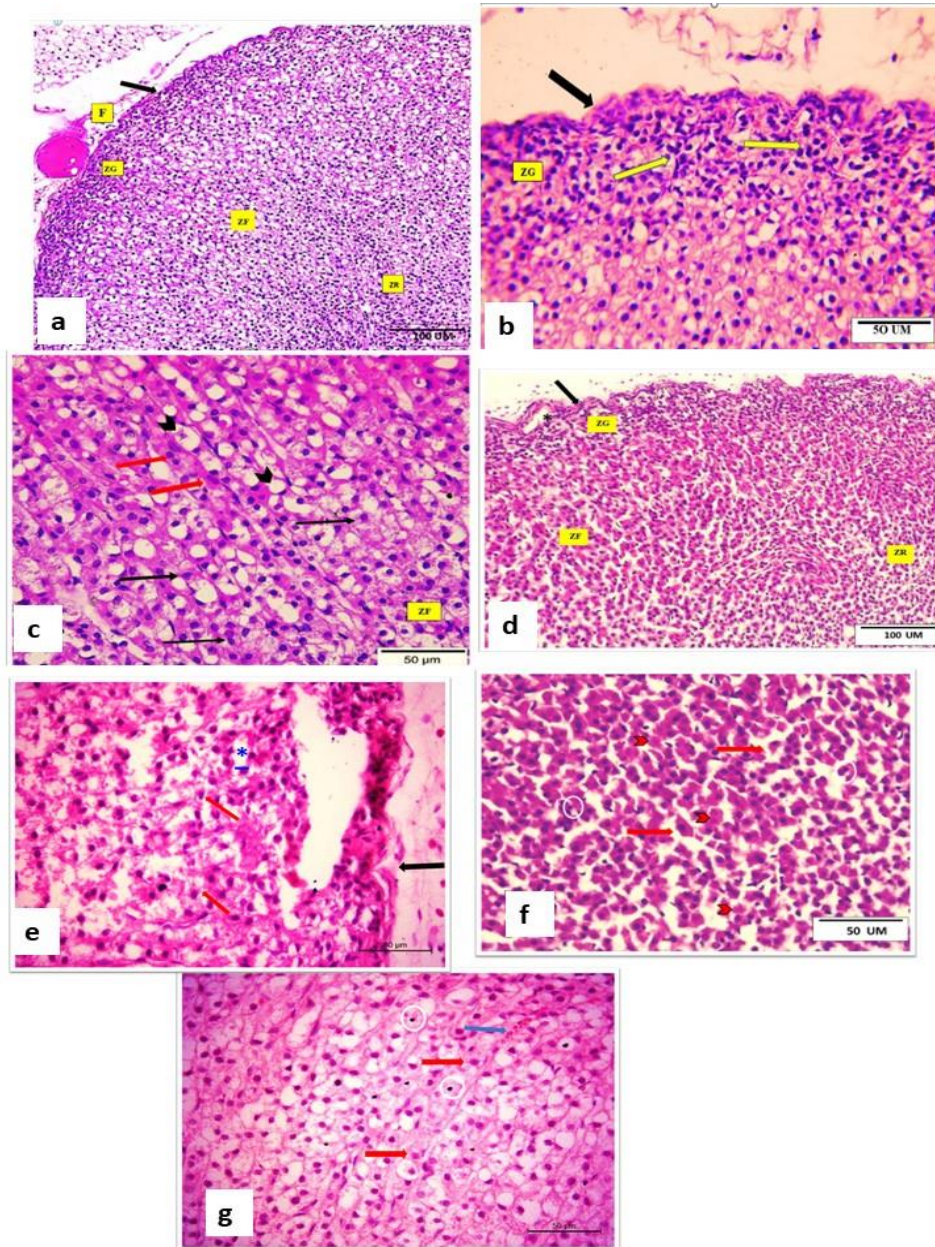


Fig. (3):(3a) A photomicrograph a section of the adrenal cortex from group IV (L-Arginine and Aspartame-treated group) showing normal architecture of the 3 zones of the cortex; ZG, ZF, ZR. The CT capsule was restored & continuous in all parts (thick black arrow) with overlying fat cells (F) (Scale bar 100 μ m) (H&E X200). (3b) A photomicrograph a section of the adrenal cortex from group IV showing a restored regular capsule (thick black arrow) (Scale bar 50 μ m) (H&E x400). ZG is arranged in round clusters of closely packed cells with vacuolated acidophilic cytoplasm and central deeply stained nuclei (thick yellow arrow) (Scale bar 50 μ m) (H&E x400). (3c) A photomicrograph of a section of the adrenal cortex from group IV

showing the zona fasciculata (ZF). The cells were arranged in longitudinal straight cords. The cells exhibited vacuolated acidophilic cytoplasm and central rounded nuclei (thin black arrows). Some binucleated cells are detected (thick red arrows, some cells were vacuolated with eccentric nuclei (arrow heads))(Scale bar 50 μm)(H&E x400). **(3d)** A photomicrograph of a section of the adrenal cortex from group V (Recovery group) showing persistence of some structural changes. The capsule appeared restored in most parts (thick black arrow); however, an area of capsular detachment was detected (*). Layers of adrenal cortex; especially zona fasciculata (ZF) showed apparent disorganization of their histo-architecture (Scale bar 100 μm)(H&E X200). **(3e)** A photomicrograph of a section of the adrenal cortex from group V revealing restored and continuous CT capsule (thick black arrow), zona glomerulosa (ZG) with irregularly arranged shrunken cells and acidophilic cytoplasm (thick yellow arrow), pyknotic nuclei (white circles), wide area of cellular shedding (S), disturbed cell membranes (thick red arrows), and widened intercellular spaces (*) in zona fasciculata (ZF) (Scale bar 50 μm)(H&E X400). **(3f)** A photomicrograph of a section of the adrenal cortex from group V revealing zona fasciculata (ZF). The cells were irregularly arranged with disruption of the normal histological architecture. Cells were shrunken with disturbed cell membranes and exhibiting deeply acidophilic cytoplasm (thick red arrows), some cells exhibited pyknotic nuclei (white circles), and others showed karyolysis (red arrow heads) (Scale bar 50 μm)(H&E X400). **(3g)** A photomicrograph of a section of the adrenal cortex from group V revealing ZF with restoration of the cell arrangement, the cells had pale acidophilic cytoplasm and central rounded nuclei (**thick** red arrows), arranged in straight cords with longitudinal blood capillaries in-between (**thick** blue arrow), but some pyknotic nuclei were still observed (white circles)(Scale bar 50 μm)(H&E X400).

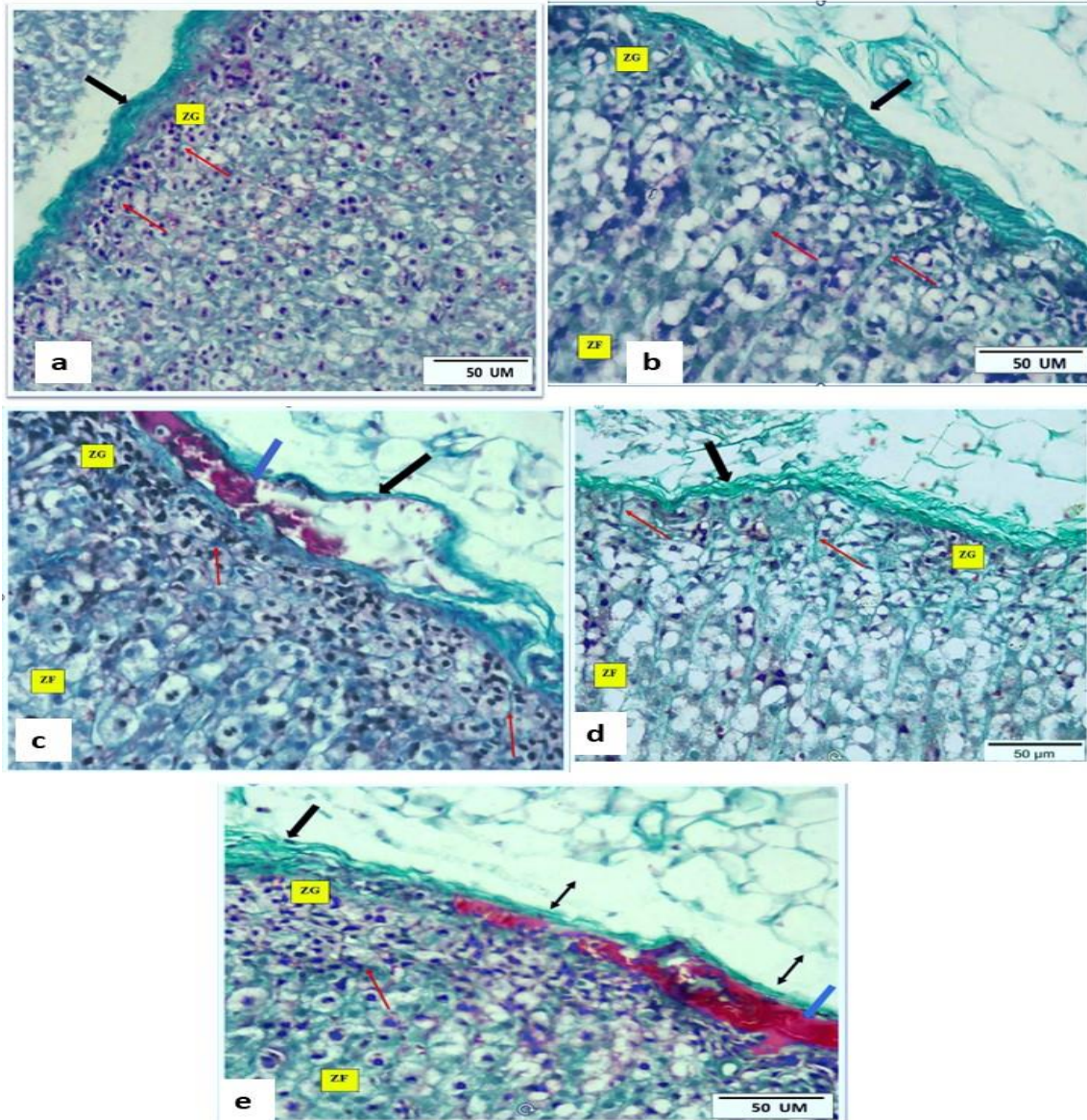


Fig. (4):(4a)A photomicrograph of Masson's trichrome stained of the adrenal cortex from group I (Control group) showing a uniform regular thick capsule (thick black arrow) surrounding the gland formed of well-packed collagen fibers, surrounding the gland, thin C.T. trabeculae extended from the capsule into the parenchyma of the gland (thin red arrows). ZG: Zona Glomerulosa.(4b) group II (L-arginine group) showing a uniform regular thick capsule (thick black arrow) surrounding the gland,thin C.T. trabeculae extended from the capsule into the parenchyma of the gland (thin red arrows). ZG: Zona Glomerulosa. ZF: Zona Fasciculata. (4c) group III (Aspartame group)showing distortion &separation of the capsule with apparent decrease in its thickness (thick black arrow),thin C.T. trabeculae extended from the capsule into

the parenchyma of the gland (thin red arrows). Notice: marked congestion in the subcapsular blood vessels (thick blue arrow). **(4d)** group IV (L-arginine and Aspartame group) showing regular, continuous C.T. capsule (thick black arrow) formed of well-packed collagen fibres with apparently increased thickness and thin C.T. trabeculae extended from the capsule into the parenchyma of the gland (thin red arrows). **(4e)** group V (Recovery group) showing relatively thick C.T. capsule formed of well packed collagen fibres in some areas (thick black arrow), while in other areas, the capsule exhibited apparent decrease in its thickness (double black arrow), and very thin C.T. trabeculae extended from the capsule into the parenchyma of the gland (thin red arrows). Notice: marked congestion in the subcapsular capillaries (thick blue arrow) (Scale bar 50 μ m) (Masson's Trichrome X400).

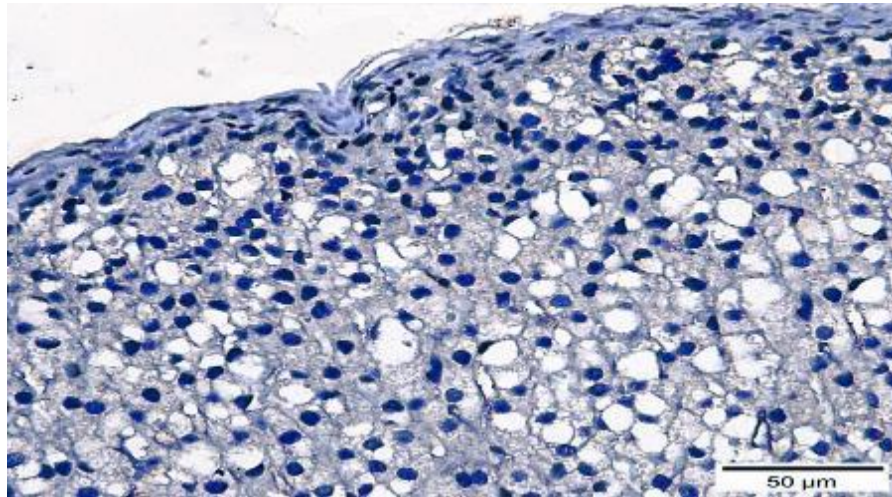


Fig. 5*: A photomicrograph of a section of the adrenal cortex for a negative control group for Caspase-3.

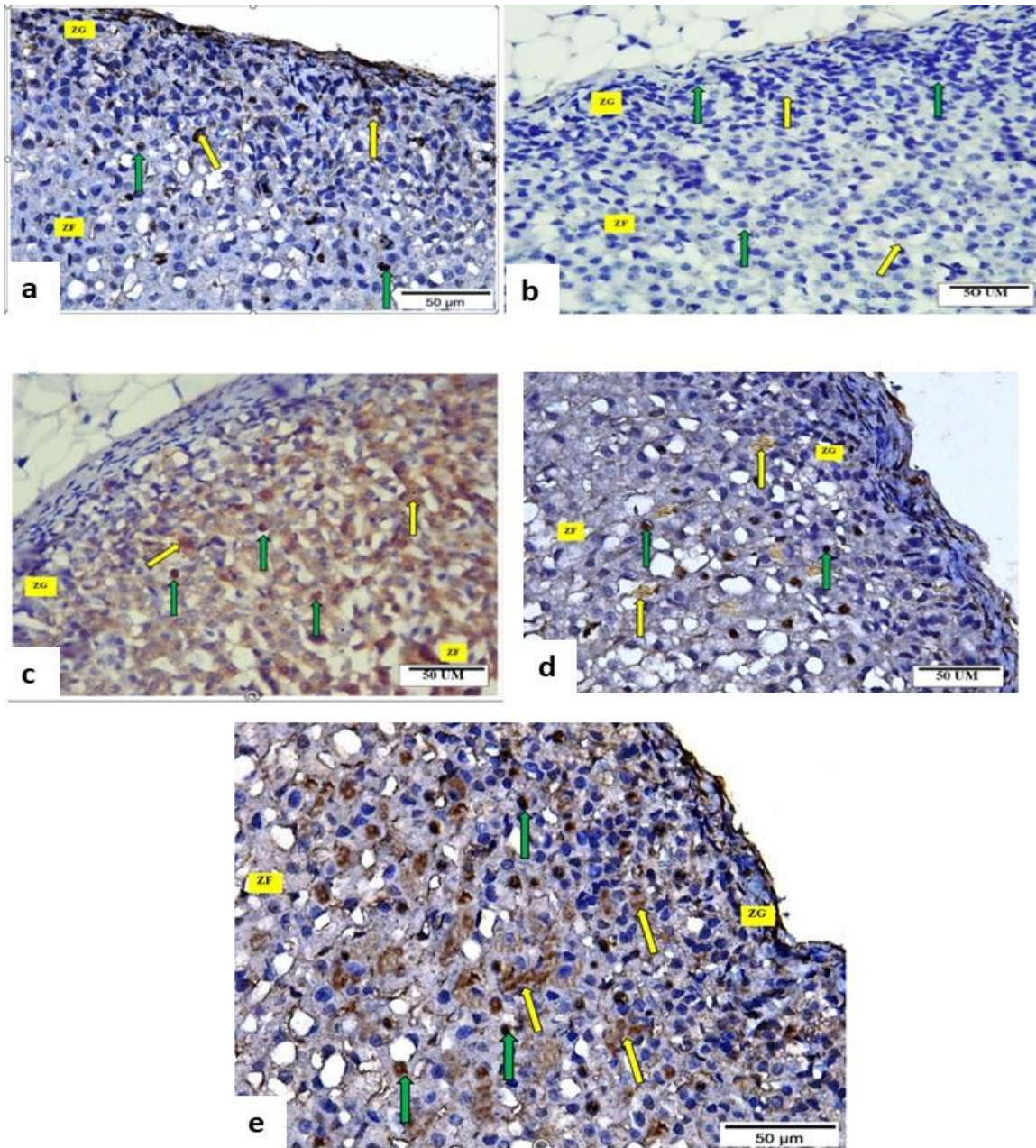


Fig. (5): (5a) A photomicrograph of a section of the adrenal cortex from group I (Control group) (5a) showing minimal positive nuclear (thick green arrows) and cytoplasmic (thick yellow arrows) reactions against caspase-3 antibodies in the cells of ZG and ZF. (5b) group II (L-arginine group) showing no positive nuclear (thick green arrows) or cytoplasmic (thick yellow arrows) reactions against caspase-3 antibodies in the cells of ZG and ZF. (5c) group III (Aspartame group) showing extensive positive nuclear (thick green arrows) and cytoplasmic (thick yellow arrows) anti-caspase-3

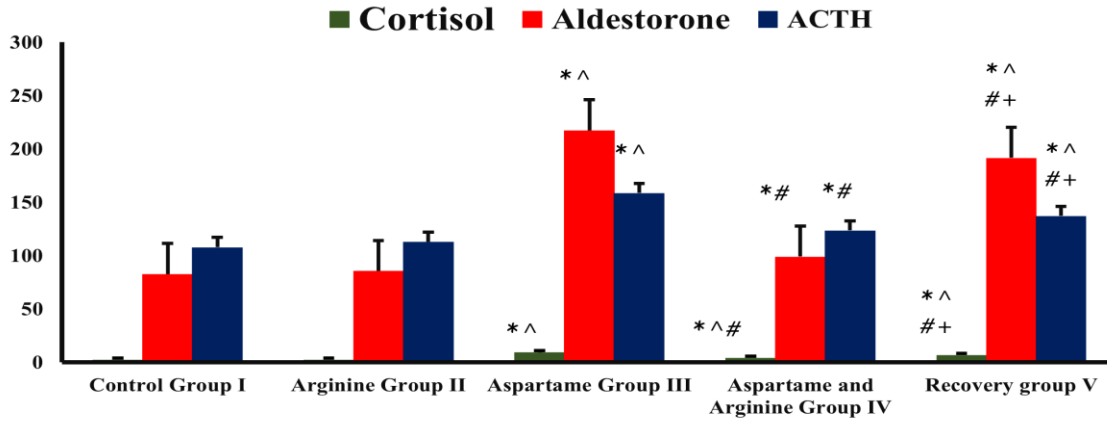
immunohistochemical reactions in the cells of ZG and ZF. (5d) group IV (L-arginine and Aspartame group) showing minimal positive nuclear (thick green arrows) and cytoplasmic (thick yellow arrows) anti-caspase-3 immunohistochemical reactions in the cells of ZG and ZF.(5e) group V (Recovery group) showing moderate positive nuclear (thick green arrows) and cytoplasmic (thick yellow arrows) anti-caspase-3 immunohistochemical reactions in the cells of ZG and ZF(Scale bar 50 μm)(Anti-Caspase-3 immune reactionX 400).

Groups	Mean ± SD		
	Cortisol (ng/ml)	Aldosterone (Pg/ml)	ACTH (Pg/ml)
Control (Group I)	2.5 ± 0.4	82.66 ±3.45	107.966 ± 6.295
L-Arginine (Group II)	2.606 ± 0.59	85.633 ±7.144	112.866 ± 2.709
Aspartame (Group III)	9.5 ± 0.3 ^{**}	217.4 ±3.386 ^{**}	158.7 ± 3.913 ^{**}
Aspartame and L-Arginine (Group IV)	4.366 ± 0.305 ^{**#}	99.133 ±1.955 ^{**#}	123.6 ± 3.629 ^{**#}
Recovery (Group V)	6.966 ± 0.23 ^{**##}	191.7 ±10.409 ^{**##}	137.2 ±5.032 ^{**##}
P- Value	0.000**	0.000**	0.000**

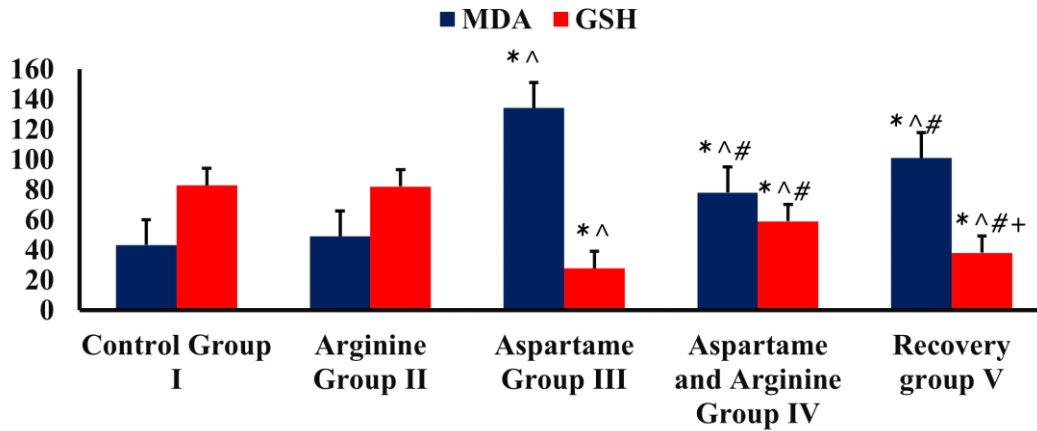
Table (1): Showing the mean ± standard deviation of serum cortisol, aldosterone, and ACTH levels in all experimental groups.

Groups	Mean ± SD	
	MDA (nmol/ml)	GSH (mmol/ml)
Control (Group I)	43.367 ±5.353	82.973 ± 5.664
L-Arginine (Group II)	49.033 ±11.469	82.133 ±2.434
Aspartame (Group III)	134.267 ± 8 ^{**}	27.9 ± 1.587 ^{**}
Aspartame and L-Arginine (Group IV)	78.2 ± 12.569 ^{**#}	59.133 ± 4.724 ^{**#}
Recovery (Group V)	101.173 ± 8.61 ^{**#}	38.233 ± 2.859 ^{**##}
P- Value	0.000**	0.000**

Table (2): Showing the mean ± standard deviation of serum MDA and GSH levels in all experimental groups.



Histogram (1): Showing the mean Cortisol, Aldosterone, and ACTH in all studied groups.



Histogram (2): Showing the mean MDA and GSH serum levels in all studied groups.

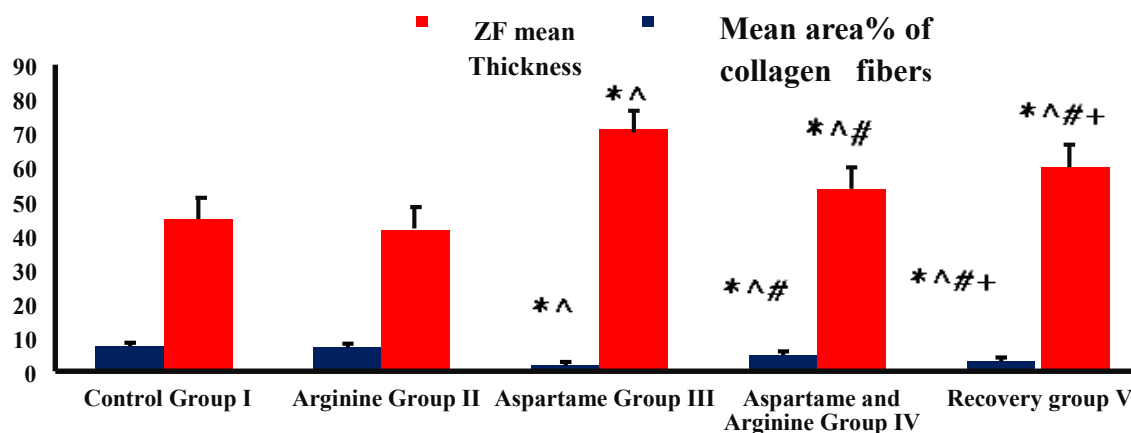
- Values are expressed as Mean ± Standard Deviation; MSD; *P- Values ≤ 0.05 are significant; **P- Values ≤ 0.001 are highly significant.

*Significant from Control Group I, ^ Significant from L-Arginine Group II, # Significant from Aspartame Group III, + Significant from Aspartame and L- Arginine Group IV at P- Values ≤ 0.05.

Groups	Mean ± SD	
	Mean area % of collagen fibres	ZF mean thickness in µm
Control (Group I)	7.228 ± 1.012	140.98 ± 1.671

Arginine (Group II)	6.947± 0.482	149.65 ± 1.019
Aspartame (Group III)	1.593 ± 0.57 ^a	278.67 ± 1.177 ^a
Aspartame and L-Arginine (Group IV)	4.697 ± 0.446 ^c	188.65 ± 1.015 ^c
Recovery (Group V)	3.16± 0.612 ^b	215 ± 3.927 ^b
P- Value	0.000**	0.000**

Table (3): Showing Means ± standard deviation of the mean area % of collagen fibres and mean thickness of ZF between tested groups.



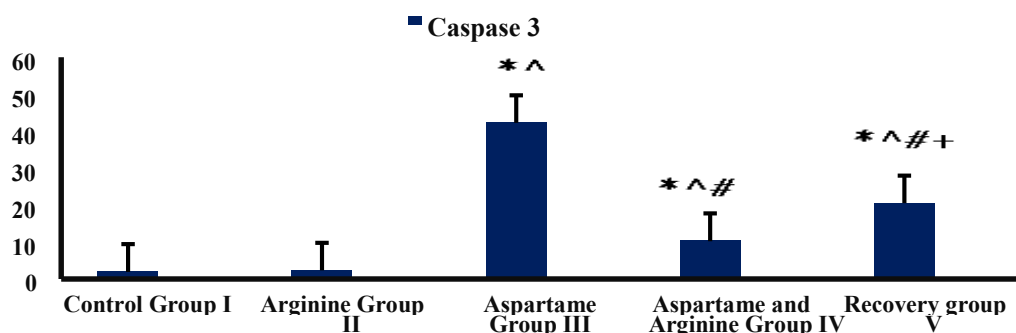
Histogram (3): Showing the mean thickness of ZF and the mean area % of collagen fibers in all studied groups.

Values are expressed as Mean ±Standard Deviation. *Significant from Control Group I, ^ Significant from Arginine Group II, # Significant from Aspartame Group III, + Significant from Aspartame and Arginine Group IV at P- Values ≤ 0.05.

Groups	Mean ± SD
	Caspase-3 mean area %
Control (Group I)	1.913 ±0.405
L-Arginine (Group II)	2.309 ±0.451
Aspartame (Group III)	42.217±1.958 ^c

Aspartame and L-Arginine (Group IV)	10.242±1.525 ^a
Recovery (Group V)	20.498±1.191 ^b
P- Value	0.000**

Table (4): Showing means ± standard deviation of immuno-scoring mean area % to Caspase 3 between tested groups.



Histogram (4): Showing the mean area % of Caspase-3 in all studied groups.

4. Discussion:

The medical and socio-economic interest recently became more concerned with the use of artificial, non-nutritive sweeteners, flavourings, and food preservatives due to the worldwide spread of type II diabetes and overweighting. In addition to their further negative impacts on human health(4).

A popular non-nutritive, synthetic sweetener is aspartame that is 200 times sweeter than the same amount of traditional households' sucrose(19).

In the intestine, aspartame is hydrolysed into, phenylalanine, aspartate, and methanol. Aspartame's metabolites are all harmful to the various organs. Consequently, the

overuse of aspartame elevates the levels of these toxic metabolites in the blood(20).

Adrenal gland is one of the organs with highest rates of blood flow in our body. So, adrenal gland is sensitive to different noxious compounds(21). The adrenal cortex

performs a crucial role in the different body activities by secreting aldosterone and cortisone hormones(1).

This study was planned to reveal adrenal cortical histological alterations after aspartame administration, as a harmful chemical stressor and to assess the possible protective effects of L-arginine.

The animals of the control and L-arginine treated groups showed normal histological features in the H&E-stained sections while the histological examination showed extensive damage to the adrenal cortex. In group III (aspartame group), the CT capsule, appeared thinner, detached in some areas, and completely shed in others. Subcapsular congestion with some inflammatory cells was noticed. Aspartame induces oxidative stress leading to cellular inflammation, the underlying cause of collagen fibres disintegration (22). Besides, Abdel-ghaffar et al., 2021 (23) denoted that aspartame can display vasculitis with degeneration of endothelial cell lining of blood vessels (24a). Additionally, an elevation in the free radicals can cause unsaturated fatty acids peroxidation in cell membranes of the vascular tissue, with subsequent blood extravasation into the subcapsular region (24b).

Aspartame administration (group III) led to marked histological changes in the cells of ZG & ZF; some cells appeared shrunken with deeply acidophilic cytoplasm, while others appeared ballooned with extensive cytoplasmic vacuolation and eccentric nuclei. Cytochrome P-450 enzyme disruption by the oxidative stress leads to cholesterol biosynthesis inhibition with lipid

droplets accumulation and development of cytoplasmic vacuolations in cells of ZF (25).

Some cells exhibited pyknotic nuclei, while others had nuclei with irregular shapes. The increased methanol following aspartame consumption results in distortions in the sizes and shapes of nuclei with other significant cellular changes, due to its impact in the tissue proteins and the nucleic acids of both mitochondrial and nuclear genetic materials (4) (15). Occasional mononuclear inflammatory cells were seen in some **Aspartame group (III)** sections that act as a defence mechanism against the oxidative tissue damage (26). Disruption of the cellular outline of ZF with formation of occasional cellular syncytium is attributed to the combined rise in the oxidative elements with lowered level of their scavengers that occurred after aspartame administration (27). Aspartame causes lipid peroxidation, which is considered as oxidative destructive process affecting the cell membranes polyunsaturated fatty acids, aiming to attenuate the membrane's fluidity and stability (20). According to (13a) cell membrane integrity is essential for adrenal steroidogenesis.

The appearance of eosinophilic homogenous exudate between cells of ZF might indicate

that aspartame treatment caused accumulation of protein secondary to cellular degeneration and adrenal gland dysfunction as denoted by **Griebschet al., 2023** ⁽¹⁹⁾who believed that aspartame-treatment induced histopathological changes in alveolar wall associated with hyaline necrosis.

Hyaline necrosis after aspartame administration was also noticed in renal tubules**(30)**.

Moreover, in the current work, the Zona Fasciculata (ZF) showed apparent increase in thickness in **aspartame group (III)**. Hyperplasia of the ZF, the most frequently affected zone of the adrenal cortex by the chemically induced damage, can be attributed to hypersecretion of ACTH from the basophilic pituitary cells in the rats treated with aspartame**(3)**. This was supported by **Morovvati et al., 2019** ⁽³¹⁾ who documented a considerable increase in the sponge cells' size, and the thickness of the fasciculata and reticularis layers after aspartame administration.

The transformation hypothesis postulated that cells would first multiply in a zone between ZG and ZF before moving outward towards the capsule and inward towards the medulla**(32)**.

H&E-stained sections of **aspartame and L-arginine-treated group (IV)** revealed notable increase in the capsule thickness. Besides, cells of both ZG and ZF restored their normal zonal organization. Restoration of adrenal cortex cellular histological organization after L-arginine administration is aided by polyamines, one of L-arginine indirect products. Polyamines involved in controlling gene transcription and translation and cell growth and proliferation according to **(13b)**.

The excess cytoplasmic vacuolation observed in the **aspartame group (III)** was apparently decreased after the administration of L-arginine resulting in significant decrease in the mean thickness of ZF in **group (IV)**. Effectiveness of L-arginine in preventing fat accumulation in adrenal cortical cells was most likely due its role in attenuating the oxidative stress which impairs the utilization of cholesterol in steroidogenesis and hence decreasing the release of ACTH and cortisol responsible for the hypertrophy of zona fasciculata (ZF) **(33)**.

In the current work, **recovery group (V)** showed incomplete improvement in the histological and biochemical aspects after 4 weeks of aspartame consumption's stoppage.

These results were supported by **Bekheet and Rady, 2020⁽¹⁵⁾** who reported that 4 weeks' cessation of aspartame consumption by the rats was insufficient to retain the sciatic nerve histological organization.

By Masson's Trichrome stain, the capsule in the **aspartame group(III)** appeared detached and distorted with decreased thickness resulting in significant decrease in the mean area % of collagen fibres compared to the other groups. This mimics the observation of **McKay et al., 2021⁽³⁴⁾** who stated that L-arginine supplementation could influence all extra cellular matrix protein secretion especially collagen I secretion from the fibroblast.

Aspartame group(III) showed up-regulation of Caspase-3 expression in the immunohistochemical stained sections, with many cells exhibiting +ve reaction in all zones of adrenal cortex. Morphometric analysis proved a significant increase in their mean area as compared with other groups. Down regulation of caspase-3 expression after L-arginine administration is due to L-arginine anti-apoptotic action by inducing the production of Heat Shock Protein-70 (HSP-70), one of the apoptosis process suppressors, and inhibiting the expression of the main apoptotic genes, such as Bcl-2 family, caspase family, and

cytochrome C (35) (36). Chronic stress might activate certain cascades of caspase activation that would ultimately evoke cellular death (37).

Aspartame acts as a stressor and causes overproduction of reactive oxygen species (ROS) that induces mitochondrial-dependent apoptosis via activation of BAX protein, which is trans-located from cytosol to mitochondria to increase the mitochondrial membrane permeability causing the liberation of the cytochromes and the activation of the caspases (38). Besides, differentiation of the adrenocortical adult progenitor stem cells in the cortex is followed by their centripetal migration that ends with their apoptosis (39).

In present work, biochemical assessment revealed statistically significant increase in MDA & significant decrease in GSH in the **aspartame group (III)** when compared to other groups. GSH reduction in **group (III)** may be due to its consumption in scavenging the O₂⁻ free radicals produced from methanol toxicity following the overuse of aspartame (40). Restoration of GSH plays a crucial role in lipid peroxides detoxification caused by the ROS (41). GSH controls tissue metabolism and protein biosynthesis, in addition to its antioxidant defence (42) (43).

Additionally, according to **Enciu et al., 2020⁽⁴⁴⁾**, the decreased activity of reduced Glutathione and increased that of MDA lasted for 42 days after the cessation of aspartame treatment. This was also reported by **Bekheet and Rady, 2020⁽¹⁵⁾** who stated that aspartame termination treatment for four weeks was insufficient for restoring the frontal cortex to its normal histological features after chronic aspartame consumption in rats. Therefore, it is crucial to note that even when daily consumption of aspartame has stopped, aspartame-induced oxidative stress may remain for prolonged periods of time and this was confirmed by the persistence of the elevated serum level of MDA in this study recovery group, after stoppage of aspartame administration for 4 weeks, when compared to the control group.

Aspartame can be considered a chemical stressor that increases the plasma level of ACTH and cortisol after its intake **(45)**. This work data revealed that aspartame treatment **(Group III)** recorded a significant elevation of serum ACTH, corticosterone, and aldosterone levels as compared to other groups. This may be attributable to methanol, a metabolite of aspartame which stimulates noradrenaline to act on the hypothalamic neurons concerned with

discharge of Corticotropin Releasing Hormone (CRH) into the hypothalamic-hypophyseal portal circulation for stimulating ACTH release from anterior pituitary **(46a)**. Finally, cortisol is secreted from the zona fasciculata when ACTH enters the peripheral systemic circulation acting on the adrenal gland **(46b) (47)**.

Despite the role of corticosteroids in regulating the miscellaneous cellular activities like homeostasis, metabolism, and inflammation, several research projects have demonstrated a link between prolonged use of corticosteroids and the incidence of variable comorbid conditions: for instance, infections, gastrointestinal ulcerations, CVS illness, Cushing's syndrome, glucose intolerance, obesity, and osteoporosis **(48)**.

At the same time there were a reduction in serum levels of ACTH, cortisol, and aldosterone in **aspartame and L-arginine treated group (IV)** when compared with aspartame group (III). Corticosterone level is direct indicator of stress level in the body so any agent able to decrease its level is actually decreasing the stress on the body. These results go hand in hand with **(1)(49)**, both discovered that L-Arginine is effective in lowering the raised stress hormone levels.

Over production of ROS can provoke sympathetic nervous system stimulation

with subsequent release of the catecholamines from adrenal medulla. The renin-angiotensin-aldosterone system (RAAS) is further activated by released catecholamines through their beta-adrenergic receptors in renal juxtaglomerular cells, ending with aldosterone release from the zona glomerulosa (50) (51). Aldosterone plays a role in controlling electrolyte and fluid homeostasis through the mineralocorticoid receptor activation, which leads to increased muscle tone of the blood vessels with subsequent increased renal absorption of water and sodium, so the primary aldosteronism is considered the leading cause of secondary hypertension(52). Excess aldosterone is considered a risk factor for cardiovascular system not only due to its association with hypertension, but also with stroke, coronary artery disease (CVD)(53). All the previous results and observations reinforce that L-arginine-mediated antioxidant effect to attenuate aspartame-induced toxicity on the adrenal cortex on the adrenal cortex of adult male albino rats.

5. Conclusion:

The present study cleared that aspartame led to histoarchitectural, immunohistochemical and biochemical changes in the adrenal cortex of rats. Through

the generation of free radicals with tissue oxidative stress. Moreover, L-arginine could protect against these changes by its antioxidant effect.

Recommendations

- It is advised to conduct further investigations on the effect of aspartame ingestion on other organs.
- The careful use and consumption of aspartame is essential.
- Additional research using prolonged periods of recovery after administration is recommended to assess the probability of complete recovery.

6. References:

1. Mahar, Y., Qamar, A., Hidayat, M., Salman, S., Chaudhry, S., & Saeeduddin, M. F. (2021). Effect Of L-Arginine And Insulin On Adrenal Gland Damaged By Streptozotocin In Albino Rats. *Journal of Ayub Medical College, Abbottabad: JAMC*, 33(1): 134-138.
2. Getabalew, M., Alemneh, T., & Zewdie, D. (2020). Review on hormonal metabolic adaptations of farm animals. *stress*, 8(9): 1037–1042.
3. Olukole, S. G., Lanipekun, D. O., Olatunmbi, E. O., & Oke, B. O. (2019). Melatonin attenuates bisphenol A-induced toxicity of the adrenal gland of

- Wistar rats. *Environmental Science and Pollution Research*, 26, 5971-5982.
4. Anbara, H., Sheibani, M. T., & Razi, M. (2020). Long-term effect of aspartame on male reproductive system: Evidence for testicular histomorphometrics, Hsp70-2 protein expression and biochemical status. *International journal of fertility & sterility*, 14(2), 91-101.
 5. Czarnecka, K., Pilarz, A., Rogut, A., Maj, P., Szymańska, J., Olejnik, Ł., & Szymański, P. (2021). Aspartame—true or false? Narrative review of safety analysis of general use in products. *Nutrients*, 13(6), 1957-1974.
 6. Hayes, J. D., Dinkova-Kostova, A. T., & Tew, K. D. (2020). Oxidative stress in cancer. *Cancer cell*, 38(2), 167-197.
 7. Liguori, I., Russo, G., Curcio, F., Bulli, G., Aran, L., Della-Morte, D., ... & Abete, P. (2018). Oxidative stress, aging, and diseases. *Clinical interventions in aging*, 13, 757-772.
 8. Vona, R., Gambardella, L., Cittadini, C., Straface, E., & Pietraforte, D. (2019). Biomarkers of oxidative stress in metabolic syndrome and associated diseases. *Oxidative medicine and cellular longevity*, 2019: 1-19.
 9. Gulcin, İ. (2020). Antioxidants and antioxidant methods: An updated overview. *Archives of toxicology*, 94(3), 651-715.
 10. Zhang, P., Li, T., Wu, X., Nice, E. C., Huang, C., & Zhang, Y. (2020). Oxidative stress and diabetes: antioxidative strategies. *Frontiers of medicine*, 14, 583-600.
 11. Ross Phan, P. (2023). L-arginine: Uses, side effects, and more, Very well Health. Available at: <https://www.verywellhealth.com/using-l-arginine-for-health-88322> (Accessed: 15 January 2024).
 12. Elbassuoni, E. A., Ragy, M. M., & Ahmed, S. M. (2018). Evidence of the protective effect of l-arginine and vitamin D against monosodium glutamate-induced liver and kidney dysfunction in rats. *Biomedicine & pharmacotherapy*, 108: 799–808.
 13. Abdel Malak, H. W., & Amin, M. A. (2018). Protective Role of L-arginine on the Suprarenal Gland of Adult Male Albino Rats Subjected to Recurrent Acute Restraint Stress: A Histological and Immunohistochemical Study. *The Egyptian Journal of Anatomy*, 41(1), 156-171.
 14. Abdelhaliem, N. G., & Mohamed, D. S. (2017). Comparative Study on The Safety of Aspartame and Stevia on The Adrenal-Pituitary Axis of Adult Male Albino Rats: Histological and Immunohistochemical

- Study. *Egyptian Journal of Histology*, 40(2), 216-225.
15. Bekheet, E. A., & Rady, H. Y. (2020). Neurotoxic effect of aspartame on the sciatic nerve of adult male albino rat and the possibility of spontaneous recovery: light and electron microscopic study. *Ain Shams Medical Journal*, 71(1), 15-30.
 16. Suvarna, K. S., Layton, C., & Bancroft, J. D. (2018). *Bancroft's theory and practice of histological techniques*, 8th edition. Chapter 9, Elsevier Health Sciences Publishing(pp. 126-138).
 17. Suvarna, K. S., Layton, C., & Bancroft, J. D. (Eds.). (2018). *Bancroft's theory and practice of histological techniques E-Book*, 8th edition, Chapter 19, Elsevier Health Sciences Publishing(pp. 337-394).
 18. Shalaby, A. M., Aboregela, A. M., Alabiad, M. A., & El Shaer, D. F. (2020). Tramadol promotes oxidative stress, fibrosis, apoptosis, ultrastructural and biochemical alterations in the adrenal cortex of adult male rat with possible reversibility after withdrawal. *Microscopy and Microanalysis*, 26(3), 509-523.
 19. Griebisch, L. V., Theiss, E. L., Janitschke, D., Erhardt, V. K. J., Erhardt, T., Haas, E. C., ... & Grimm, H. S. (2023). Aspartame and Its Metabolites Cause Oxidative Stress and Mitochondrial and Lipid Alterations in SH-SY5Y Cells. *Nutrients*, 15(6), 1467.
 20. Hassen, E. Z., Ibrahim, N. E., & El-Shal, A. S. (2019). The Effect of Long Term Administration of Aspartame on the Sciatic nerve of adult male albino rats and the Possible Therapeutic Role of Ozone (Histological and Biochemical Study). *Egyptian Journal of Histology*, 42(1), 191-201.
 21. EL Tahawy, N. F. G., & Abozaid, S. M. M. (2019). The possible structural changes in the adrenal gland cortex after induction of hepatic ischemia–reperfusion injury in male albino rats: Light and electron microscopic study. *Journal of Cellular Physiology*, 234(9), 15487-15495.
 22. Umbayev, B., Askarova, S., Almabayeva, A., Saliev, T., Masoud, A. R., & Bulanin, D. (2020). Galactose-induced skin aging: the role of oxidative stress. *Oxidative Medicine and Cellular Longevity*, 2020,1-15.
 23. Abdel-ghaffar, S. K., Adly, M. A., El-Sayed, M. F., & Abd-Elsamei, W. M. (2021). Protective effects of some antioxidants against long-term intake of aspartame toxicity on liver and kidney: biochemical and histopathological approach in rats. *The Journal of Basic and Applied Zoology*, 82(1), 1-9.

24. Azez, O. H., Baker, S. A., Abdullah, M. A., & Nabi, R. K. (2023). Histopathological and the Dose Depended Effects of Aspartame toxicity on Liver and Kidney of Rats. *Journal of Applied Veterinary Sciences*, 8(2), 16-22.
25. Sadek, M. T., El-Abd, S. S., & Ibrahim, M. A. (2020). Effect of Chronic Unpredictable Mild Stress on Adrenal Cortex of Adult Rat and The Possible Protective Role of Licorice Extract: A Histological and Immunohistochemical study. *Egyptian Journal of Histology*, 44(4), 887-901.
26. Ali, O. S. M., Amin, N. E. D., Abdel Fattah, S. M., & Abd El-Rahman, O. (2020). Ameliorative effect of kefir against γ -irradiation induced liver injury in male rats: Impact on oxidative stress and inflammation. *Environmental Science and Pollution Research*, 27, 35161-35173.
27. Vural, P., Kabaca, G., Firat, R. D., & Degirmecioglu, S. (2017). Administration of selenium decreases lipid peroxidation and increases vascular endothelial growth factor in streptozotocin induced diabetes mellitus. *Cell Journal (Yakhteh)*, 19(3), 452.
28. Ito, F., Sono, Y., & Ito, T. (2019). Measurement and clinical significance of lipid peroxidation as a biomarker of oxidative stress: oxidative stress in diabetes, atherosclerosis, and chronic inflammation. *Antioxidants*, 8(3): 72-100.
29. Moftah, O. M. Y., Gadallah, A. A., Elemam, S. I. A., & El-Sayyad, H. I. H. (2020). Impairment of Hepatic, Cardiac and Lung Tissues in Aspartame Treated Male Wistar Albino Rats. *East African Scholars Journal of Medical Sciences*, (3)2: 41-46.
30. El Haliem, N. G., & Mohamed, D. S. (2011). The effect of aspartame on the histological structure of the liver and renal cortex of adult male albino rat and the possible protective effect of Pimpinella anisum oil. *Egyptian Journal of Histology*, 34(4), 715-726.
31. Morovvati, H., Anbara, H., Sheibani, M. T., Koohi, M. K., & Hasanzadeh, A. (2019). The effect of long-term exposure to aspartame on histomorphometric and histochemical adrenal gland in adult NMRI mice. *Armaghane Danesh*, 24(2): 150-169.
32. Guo, Y., Zhang, L., Yao, X., Tong, R., Cheng, C., Zhang, T., Wang, S., & Yang, H. G. (2019). Effects of nitric oxide on steroidogenesis and apoptosis in goat

- luteinized granulosa cells. *Theriogenology*, 126: 55-62.
33. Ali, A. F., & Badawy Khair, N. S. (2023). Effect of induced hepatic ischemia–reperfusion on the adrenal cortex of adult male albino rats and the possible protective role of L-arginine: Biochemical, histological and immunohistochemical study. *Egyptian Journal of Histology*, 46(1), 206-220.
34. McKay, T. B., Priyadarsini, S., Rowsey, T., & Karamichos, D. (2021). Arginine Supplementation Promotes Extracellular Matrix and Metabolic Changes in Keratoconus. *Cells*, 10 (8): 2076-2088.
35. Attia, H., Fadda, L., Al-Rasheed, N., Al-Rasheed, N., & Maysarah, N. (2020). Carnosine and l-arginine attenuate the downregulation of brain monoamines and gamma aminobutyric acid; reverse apoptosis and upregulate the expression of angiogenic factors in a model of hemic hypoxia in rats. *Naunyn-Schmiedeberg's Archives of Pharmacology*, 393(3): 381-394.
36. Darband, S. G., Sadighparvar, S., Yousefi, B., Kaviani, M., Mobaraki, K., & Majidinia, M. (2020). Combination of exercise training and L-arginine reverses aging process through suppression of oxidative stress, inflammation, and apoptosis in the rat heart. *Pflügers Archiv-European Journal of Physiology*, 472(2): 169-178.
37. Anbara, H., Kian, M., Darya, G. H., & Sheibani, M. T. (2022). Longterm intake of aspartame induced cardiovascular toxicity is reflected in altered histochemical parameters, evokes oxidative stress, and trigger P53 dependent apoptosis in a mouse model. *International Journal of Experimental Pathology*, 103(6): 252-262.
38. Jan, R. (2019). Understanding apoptosis and apoptotic pathways targeted cancer therapeutics. *Advanced pharmaceutical bulletin*, 9(2): 205-219.
39. Finco, I., Mohan, D. R., Hammer, G. D., & Lerario, A. M. (2019). Regulation of stem and progenitor cells in the adrenal cortex. *Current opinion in endocrine and metabolic research*, 8: 66-71.
40. Ali, W. A. G., Mohammed, S. A., Abdullah, E. M., & Salah ElDeen, E. M. (2019). Aspartame: basic information for toxicologists. *Sohag Medical Journal*, 23(2): 47-51.
41. Karpets, Y. V., Kolupaev, Y. E., & Shkliarevskiy, M. A. (2021). Functional interaction of hydrogen sulfide with nitric oxide, calcium, and reactive oxygen

- species under abiotic stress in plants. *Hydrogen Sulfide and Plant Acclimation to Abiotic Stresses*, 2021(1): 31-57.
42. He, H., Oo, T. L., Huang, W., He, L. F., & Gu, M. (2019). Nitric oxide acts as an antioxidant and inhibits programmed cell death induced by aluminum in the root tips of peanut (*Arachis hypogaea* L.). *Scientific Reports*, 9(1): 1-12.
43. Egbunu, A. C. C., & Elendu, D. S. (2021). Alterations in brain histomorphology and some homogenate antioxidant bio-pointers in L-arginine co-exposed aspartame assaulted rats. *Animal Research International*, 18(2): 4116-4124.
44. Enciu, R. R., Trus, C., & Ungurianu, S. (2020). Aspartame Consumption Increases Glutathione Peroxidase Level and Depression-Like Behavior in Rats. *REV. CHIM*, 71: 247-253.
45. Choudhary, A. K., & Lee, Y. Y. (2018). Neurophysiological symptoms and aspartame: What is the connection?. *Nutritional neuroscience*, 21(5): 306-316.
46. Collison, K. S., Inglis, A., Shibin, S., Saleh, S., Andres, B., Ubungen, R., Thiam, J., Mata, P., & Al-Mohanna, F. (2018). Effect of developmental NMDAR antagonism with CGP 39551 on aspartame-induced hypothalamic and adrenal gene expression. *PloS one*, 13(3): e0194416-e0194447.
47. Clark, K. A., Jacob, E. B., MohanKumar, P. S., & MohanKumar, S. M. (2019). Leptin and HPA axis activity in diabetic rats: effects of adrenergic agonists. *Brain Research*, 1707: 54-61.
48. Herman, O. M., Herasymiuk, I. Y., & Fedoniuk, L. Y. (2021). Character and specifics of the structural alteration of the parenchyma and bloodstream of the testes of white rats with prolonged administration of high doses of prednisolone. *Wiad Lek*, 74(12): 3147-3151.
49. Yang, J. Y., Zhang, Y. F., Li, Y. X., Meng, X. P., & Bao, J. F. (2018). l-arginine protects against oxidative damage induced by T-2 toxin in mouse Leydig cells. *Journal of biochemical and molecular toxicology*, 32(10): e22209-e22217.
50. Touyz, R. M., Rios, F. J., Alves-Lopes, R., Neves, K. B., Camargo, L. L., & Montezano, A. C. (2020). Oxidative stress: a unifying paradigm in hypertension. *Canadian Journal of Cardiology*, 36(5): 659-670.

51. Gideon, A., Sauter, C., Fieres, J., Berger, T., Renner, B., & Wirtz, P. H. (2020). Kinetics and interrelations of the renin aldosterone response to acute psychosocial stress: a neglected stress system. *The Journal of Clinical Endocrinology & Metabolism*, 105(3): e762-e773.
52. Freeman, M. W., Bond, M., Murphy, B., Hui, J., & Isaacsohn, J. (2023). Results from a phase 1, randomized, double-blind, multiple ascending dose study characterizing the pharmacokinetics and demonstrating the safety and selectivity of the aldosterone synthase inhibitor baxdrostat in healthy volunteers. *Hypertension Research*, 46(1): 108-118.
53. Ferreira, N. S., Tostes, R. C., Paradis, P., & Schiffrin, E. L. (2021). Aldosterone, inflammation, immune system, and hypertension. *American Journal of Hypertension*, 34(1): 15-27.

